

Debris Flow Hazard Analysis Toward The Implementation Of Mitigation Measures

by Anisa Nur Amalina

Submission date: 04-Nov-2022 10:05AM (UTC+0700)

Submission ID: 1944071342

File name: 2022-Amalina-Debris-Geomate.pdf (8.75M)

Word count: 9021

Character count: 47519



Source details

International Journal of GEOMATE

Scopus coverage years: from 2011 to Present

Publisher: GEOMATE International Society

ISSN: 2186-2982 E-ISSN: 2186-2990

Subject area: Environmental Science: Environmental Engineering Agricultural and Biological Sciences: Soil Science

Earth and Planetary Sciences: Geotechnical Engineering and Engineering Geology

Engineering: Building and Construction

Source type: Journal

[View all documents >](#) [Set document alert](#) [Save to source list](#) [Source Homepage](#)

[CiteScore](#) [CiteScore rank & trend](#) [Scopus content coverage](#)

CiteScore 2021 ⓘ
1.7

SJR 2021 ⓘ
0.360

SNIP 2021 ⓘ
0.721

i Improved CiteScore methodology ✕

CiteScore 2021 counts the citations received in 2018-2021 to articles, reviews, conference papers, book chapters and data papers published in 2018-2021, and divides this by the number of publications published in 2018-2021. [Learn more >](#)

CiteScore 2021 ▾

$$1.7 = \frac{2,389 \text{ Citations 2018 - 2021}}{1,428 \text{ Documents 2018 - 2021}}$$

Calculated on 05 May, 2022

CiteScoreTracker 2022 ⓘ

$$1.6 = \frac{1,956 \text{ Citations to date}}{1,231 \text{ Documents to date}}$$

Last updated on 05 October, 2022 • Updated monthly

CiteScore rank 2021 ⓘ

Category	Rank	Percentile
Environmental Science	#106/173	39th
Environmental Engineering		
Agricultural and Biological Sciences	#89/145	38th
Soil Science		

[View CiteScore methodology >](#) [CiteScore FAQ >](#) [Add CiteScore to your site ↗](#)


International Journal of GEOMATE

COUNTRY	SUBJECT AREA AND CATEGORY	PUBLISHER	H-INDEX
Japan 	Agricultural and Biological Sciences Soil Science Earth and Planetary Sciences Geotechnical Engineering and Engineering Geology Engineering Building and Construction Environmental Science Environmental Engineering	GEOMATE International Society	21

PUBLICATION TYPE	ISSN	COVERAGE	INFORMATION
Journals	21862982, 21862990	2011-2021	Homepage How to publish in this journal editor@geomatejournal.com

SCOPE

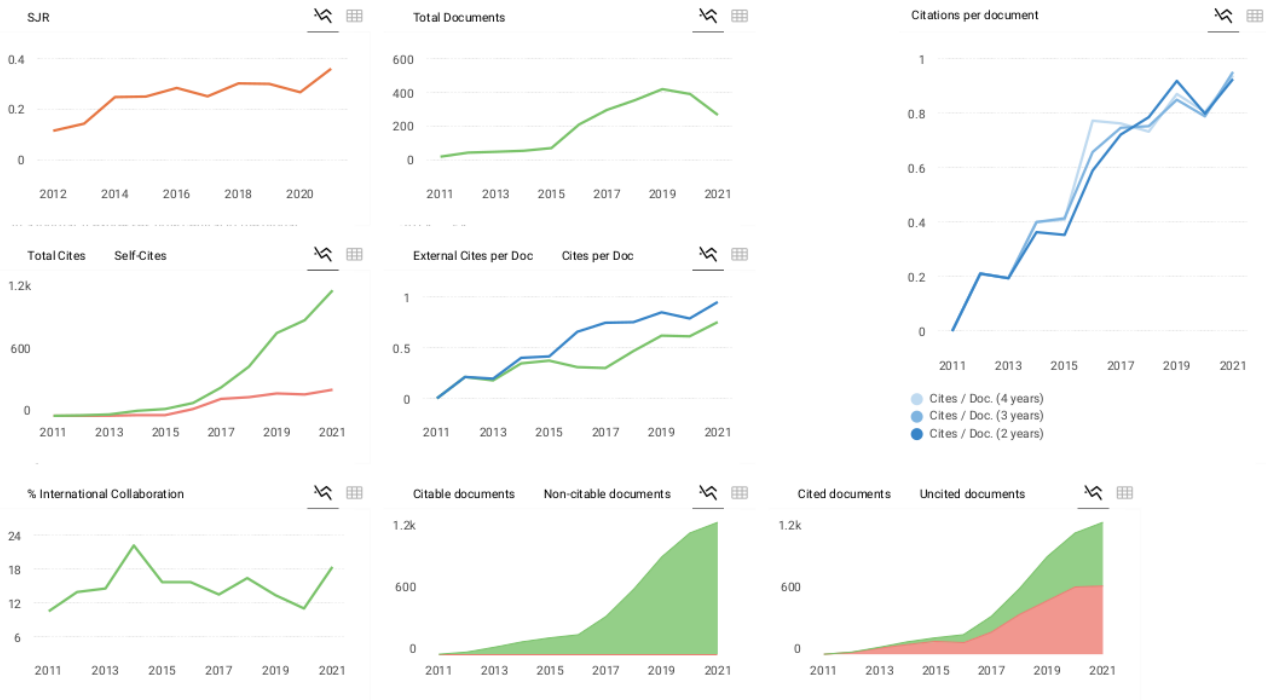
The journal aims to become an efficient mean of publishing and distributing high quality information from the researchers, scientists and engineers. The main scopes are as follows: Advances in Composite Materials- Computational Mechanics- Foundation and Retaining Walls- Slope Stability- Soil Dynamics- Soil-Structure Interaction- Pavement Technology- Tunnels and Anchors- Site Investigation and Rehabilitation- Ecology and Land Development- Water Resources Planning- Environmental Management - Public Health and Rehabilitation- Earthquake and Tsunami Issues- Safety and Reliability- Geo-Hazard Mitigation- Case History and Practical Experience- Others

 Join the conversation about this journal

Quartiles

FIND SIMILAR JOURNALS

1 Journal of The Institution of Engineers (India): Series A IND <div style="text-align: center;">30% similarity</div>	2 Advances in Materials Science and Engineering USA <div style="text-align: center;">29% similarity</div>	3 Journal of Testing and Evaluation USA <div style="text-align: center;">28% similarity</div>	4 Iranian Journal of Science and Technology - CHE <div style="text-align: center;">28% similarity</div>	5 Open Civil Engineering Journal ARE <div style="text-align: center;">27% similarity</div>
--	--	--	--	---



← Show this widget in your own website

International Journal of GEOMATE

Q3 Building and Construction best quartile

SJR 2021 0.36

powered by scimagojr.com

Just copy the code below and paste within your html code:

SCImago Graphica

Explore, visually communicate and make sense of data with our **new data visualization tool**.

Metrics based on Scopus® data as of April 2022

D dwikoranto 1 year ago

Thank you, I started joining to get information about journals.

reply

Melanie Ortiz 1 year ago

Dear Sir/Madam, welcome and thanks for your participation! Best Regards, SCImago Team

N nahla salim 2 years ago

Dear Sir

I would like to publish in Geotechnical branch and I would like to know how long it will take for publishing

Thank you very much

reply



[Home](#) / [Editorial Team](#)

Editorial Team

Editor-in-Chief

Prof. Dr. Zakaria Hossain, Mie University, Japan

Executive Editor-in-Chief

E/Prof. Dr. Takamitsu Kajisa, Mie University, Japan

Associate Editor-in-Chief

Associate Prof. Dr. John Victor Smith, RMIT University, Australia

Prof. Dr. Fumio Tatsuoka, Tokyo
University of Science, Japan

Prof. Dr. Sai Vanapalli, University of
Ottawa, Canada

Prof. Dr. Ian Jefferson, University of
Birmingham, United Kingdom

Prof. Dr. Mounir Bouassida, National
School of Engineering of Tunis

Prof. Dr. Bujang B.K. Huat, University
Putra Malaysia, Malaysia

Prof. Dr. Nemy Banthia, University of British
Columbia, Canada

Prof. Dr. Toshinori Sakai, Mie University,
Japan

Prof. Dr. Valeriy Perminov, Tomsk
Polytechnic University, Russia

Prof. Dr. Jing-Cai Jiang, University of Tokushima,
Japan

Prof. Dr. Lilia Robles Austriaco, Angles
University Foundation, Philippines

Prof. Dr. Muhammad Ibn Ibrahimy,
International Islamic University, Malaysia

Prof. Dr. Shamsul I. Chowdhury, Roosevelt
University, USA

Prof. Dr. Isabel Pinto, University of
Coimbra, Portugal

Prof. Dr. Mark Jaksa, University of
Adelaide, Australia

Prof. Dr. Kaneco Satoshi, Mie University, Japan

Prof. Dr. Junichiro Takeuchi, Kyoto
University, Japan

Prof. Dr. Ranjith Pathegama
Gamage, Monash University, Australia

Prof. Dr. Kingshuk Roy, Nihon University, Japan

Prof. Dr. Md. Shahin Hossain, Islamic
University of Technology, Bangladesh

Prof. Dr. Pedro Arrua, Universidad
Tecnológica Nacional, Argentina

Prof. Dr. Miguel A. Pando, Drexel University,
Philadelphia, USA

Prof. Dr. Suksun Horpibulsuk, Suranaree
University of Technology, Thailand

Prof. Dr. Musharraf Zaman, University of
Oklahoma, USA

Prof. Dr. Rafiqul Tarefder, University of New
Mexico, USA

Dr. Stefano Stacul, University of Pisa,
Italy

Prof. Dr. Basir Mir, National Institute of
Technology Srinagar, India

Prof. Dr. Lily Surayya Eka, State Islamic
University Syarif Hidayatullah Jakarta, Indonesia



Vol. 23 No. 95 (2022): July 2022

Published: 2022-07-01

Articles

COMPARATIVE STUDY OF FLEXURAL PERFORMANCE OF GEOPOLYMER AND PORTLAND CEMENT CONCRETE BEAM USING FINITE ELEMENT ANALYSIS

Muhammad Sigit Darmawan, Yuyun Tajunnisa, Priyo Suprobo, Wahyuniarsih Sutrisno, Muhammad Wildan Aziz

1-9



Abstract View : 162

PDF downloads: 172

SUSTAINABLE IMPROVEMENT OF BENTONITE CLAY CHARACTERISTICS BY ADDING PULVERIZED WASTE GLASS

Madhat Shakir Al-Soud, Sabah Hassan Fartosy, Aqeel Raheem Jabur, Muhamnd Waleed Majeed, Huda M. Madhloom, Nadhir Al-Ansari

10-19



Abstract View : 148

PDF downloads: 124

UTILIZATION OF COIR FIBERS TO IMPROVE THE BEARING CAPACITY AND TENSILE STRENGTH OF EXPANSIVE CLAY

Anita Widianti, Angesta Artha Bhakti Negara, Tjokro Seigia Elmino, Lazuardi Ramadhani

20-26



Abstract View : 108

PDF downloads: 115

THE OPTIMIZATION OF OPERATIONAL PATTERNS FOR CIPANUNJANG-CILEUNCA CASCADE RESERVOIR USING CONTINUOUS MODELS

Mariana Marselina, Arwin Sabar, Arini Mushfiroh

27-36



Abstract View : 93

PDF downloads: 44

THE PROMISING POTENTIAL OF SIDOARJO HOT MUD AS ADDITIONAL MATERIAL FOR CONCRETE LINING PRODUCTION

Lies Kurniawati Wulandari, I Wayan Mundra, Maranatha Wijayaningtyas

37-44

PDF

Abstract View : 88

PDF downloads: 77

DEBRIS FLOW HAZARD ANALYSIS TOWARD THE IMPLEMENTATION OF MITIGATION MEASURES

Teuku Faisal Fathani, Wahyu Wilopo, Anisa Nur Amalina, Avantio Pramaditya

45-56

PDF

Abstract View : 138

PDF downloads: 98

MACHINE LEARNING MODELS TO GENERATE A SUBSURFACE SOIL PROFILE: A CASE OF MAKATI CITY, PHILIPPINES

Joemel Galupino, Jonathan Dungca

57-64

PDF

Abstract View : 102

PDF downloads: 84

THE MOST SUITABLE SEISMIC STRUCTURAL SYSTEMS IN HIGH-RISE REINFORCED CONCRETE BUILDINGS

Odai Hasan Fawzi Masheh, Mohammed Salman Al-lami

65-72

PDF

Abstract View : 71

PDF downloads: 52

PERFORMANCE OF A WIRELESS SENSOR ADOPTED IN MONITORING OF CONCRETE STRENGTH

Yelbek Uteпов, Assel Tulebekova, Aliya Aldungarova, Shyngys Zharassov, Yerlan Sabitov

73-80

PDF

Abstract View : 49

PDF downloads: 55

DYNAMICS OF PARK USERS DURING COVID-19 PANDEMIC: A CASE STUDY OF SHIKISHIMA PARK IN MAEBASHI

Xingyu Tao, Shinya Tsukada, Tetsuo Morita, Toshikazu Nishio

81-88

PDF

Abstract View : 38

PDF downloads: 25

ANTIBACTERIAL ACTIVITY OF LIQUID SMOKE POWDER FROM RICE HUSK

Muriady, Hesti Meilina, Muhammad Faisal

89-96



PDF

Abstract View : 75

PDF downloads: 58

EVALUATION OF MUD SETTLING POND PERFORMANCE IN A SALT POND ENVIRONMENT IN LOSARANG DISTRICT, REGENCY OF INDRAMAYU, WEST JAVA, INDONESIA

Harman Ajiwibowo, Munawir B. Pratama

97-103



PDF

Abstract View : 71

PDF downloads: 31

AN ASSESSMENT OF FLOOD HAZARDS DUE TO THE BREACH OF THE MANGGARAI FLOOD GATE

Tri Nugraha Adi Kesuma, Muhammad Syahril Badri Kusuma, Mohammad Farid, Arno Adi Kuntoro, Harkunti Pertiwi Rahayu

104-111



PDF

Abstract View : 89

PDF downloads: 77

EXPERIMENTAL INVESTIGATION ON THE ULTIMATE CAPACITY OF RECTANGULAR REINFORCED HYBRID CONCRETE COLUMNS UNDER AXIAL LOAD

Alyaa Hussein Mohammed, Layla Ali Ghalib Yassin, Marawan Mohammed Hamid

112-118



PDF

Abstract View : 57

PDF downloads: 49

WATER BALANCE ANALYSIS AND ZERO ARTIFICIAL RUN-OFF (ZARo) CONCEPT IN METROPOLITAN BANDUNG AREA, WEST JAVA PROVINCE

Imam Priyono, Deny Juanda Puradimaja, Budi Sulistijo, Muhammad Syahril Badri Kusuma

119-126



PDF

Abstract View : 46

PDF downloads: 61

INFLUENCE OF HOOKED-END STEEL FIBERS ON FLEXURAL BEHAVIOR OF STEEL FIBER REINFORCED SELF-COMPACTING CONCRETE (SFRSCC)

Saloma, Faiz Sulthan

127-135



PDF

Abstract View : 82

PDF downloads: 51

PREDICTION OF BLAST-INDUCED THE AREA OF THE TUNNEL FACE IN UNDERGROUND EXCAVATIONS USING FUZZY SET THEORY ANFIS AND ARTIFICIAL NEURAL NETWORK ANN

Chi Thanh Nguyen, Ngoc Anh Do, Van Vi Pham, Phuong Thuy Nguyen, Gospodarikov Alexandr

136-143



PDF

Abstract View : 148

PDF downloads: 57

EVOLUTION STUDY OF THE PAVEMENT STRUCTURAL INDICATOR BASED ON EVENNESS AND DEFLECTION RESULTS USING A GIS TOOL MAPPING

Mohammed Amine Mehdi, Toufik Cherradi, Azzeddine Bouyahyaoui, Said El Karkouri, Ahmed Qachar

144-153



PDF

Abstract View : 57

PDF downloads: 48

MULTI-OBJECTIVE OPTIMIZATIONS OF HYDROELECTRIC EXPLOITATION USING DYNAMIC PROGRAMS IN CITARUM CASCADE RESERVOIRS

Eddy Iskandar Muda Nasution, Arwin Sabar, Indah Rachmatiah Siti Salami, Dyah Marganingrum

154-161



PDF

Abstract View : 44

PDF downloads: 37

EFFECTS OF POLYETHYLENE TEREPHTHALATE (PET) PLASTICS ON THE MECHANICAL PROPERTIES OF FLY ASH CONCRETE

Mary Ann Adajar, Irene Olivia Ubay-Anongphouth

162-167



PDF

Abstract View : 99

PDF downloads: 71

[Submit your paper](#)

[Journal Menu](#)

[Guide for Authors](#)

Paper Template, Copyright, etc.

Aims and Scope

Publication Ethics

Conferences

Reviewer Application and Policy

Fee and Pay Link

Scopus Indexed



Information

[For Readers](#)

[For Authors](#)

[For Librarians](#)

Address:

Prof. Dr. Zakaria Hossain
Mie University, Japan

Contact Info:

editor@geomatejournal.com

Information :

[Authors](#)

[Terms of Use](#)

[Privacy Policy](#)

DEBRIS FLOW HAZARD ANALYSIS TOWARD THE IMPLEMENTATION OF MITIGATION MEASURES

*Teuku Faisal Fathani¹, Wahyu Wilopo², Anisa Nur Amalina³, and Avantio Pramaditya¹

¹Department of Civil and Environmental Engineering, Faculty of Engineering, Universitas Gadjah Mada, Indonesia; ²Department of Geological Engineering, Faculty of Engineering, Universitas Gadjah Mada, Indonesia; ³Department of Civil Engineering, Faculty of Civil Engineering and Planning, Islamic University of Indonesia, Indonesia

*Corresponding Author, Received: 9 Jan. 2022, Revised: 8 June 2022, Accepted: 17 June 2022

ABSTRACT: A massive debris flow occurred on 28 April and 3 May 2016 in Beriti Hill, Bengkulu Province, Indonesia. The debris flow carried 4.3 million cubic meters of sediment materials containing 1-2 m diameter boulders that damaged roads, bridges, and geothermal facilities. This study assesses the debris flow hazard through comprehensive field investigation and laboratory testing and analyses the effectiveness of proposed mitigation measures against the destructive energy of the debris flow. A closed-type conduit Sabo dam is proposed as a countermeasure. The design of the Sabo dam considered the engineering geology, hydrologic and hydraulic, and geotechnical aspects. The hydrologic analysis used Synthetic Unit Hydrograph, which was continued by flood analysis using HEC-RAS. The geotechnical analysis was conducted to determine the Sabo dam stability utilizing the field and laboratory test data. The analysis shows that without a Sabo dam, the debris flows were distributed to a larger area downstream and destroyed the structure of the old bridge. The impacted area reduced significantly when the Sabo dam was implemented.

Keywords: Sabo bridge, Volcanic River, Hydrological analysis, Dam stability, Countermeasures

1. INTRODUCTION

Debris flows are natural disasters that can cause morphological change, severe damage, and casualties to the surrounding area. Debris flows are found in the mountainous area and consist of fully saturated mixtures of water, sediment, and debris [1-3]. It is commonly initiated upstream of a mountainous area when unconsolidated material becomes saturated and unstable [4]. Debris flows are widely recognized as geomorphic processes in mountainous areas [5,6]. It starts high on the hill slope and travels down through the channel or gully while increasing the volume by entraining materials from the channels. The size of particles in debris flows varies widely, ranging from clay to boulder [7].

Numerous cases of intense rainfall-triggered debris flow have been well documented, causing structural damages and casualties [8,9,10]. The impact of debris flows disasters is heavily linked to the community's vulnerability to the hazards [11]. The lack of disaster risk reduction capacities in developing countries results in a gap between an increased risk of natural hazards and the risk perception by communities [12]. Engineering mitigation strategies also play an essential role in reducing disaster risk. The commonly adopted engineering strategies are not applicable for all types of debris flow catchment areas. Mountain debris flows characterized by steep river slopes,

heavy rain events, and large amounts of loose material, for example, need a specific strategy to be effective [13]. Therefore, it is crucial to study the effectiveness of debris flow mitigation strategies.

One of the structural measures used to prevent and control debris flows is dams. The continuous development of engineering technology and debris flow disaster prevention and control makes dams widely used in disaster management [14,15]. Sabo dams are among the most effective structural countermeasures to control the debris flow [2,4,16,17]. Sabo dams are usually built in mountainous areas with abundant bulk materials and high-intensity rainfall. The construction of Sabo dams aims to effectively reduce the amount of debris flow by capturing and trapping solid particles [15,18] and can be distinguished into closed and open-type dams [19]. Closed-type Sabo dams effectively trap the debris materials and contain a channelized debris flow. In contrast, open-type Sabo dams are designed to temporarily hold the debris materials (medium to large size debris) and provide the sediment routing to allow harmless materials to flow downstream [20,21].

This study aims to assess the risk of debris flows in mountainous areas with high-intensity rainfalls and assess the effectiveness of mitigating strategies. A thorough hazard analysis was carried out to identify the potential hazard in the area. It is then continued by designing a mitigation measure to reduce the effect of debris flow hazards. In this

study, a closed-type conduit Sabo dam can also be utilized as a bridge for the access road in the geothermal exploration area is proposed and evaluated.

2. LANDSLIDE INDUCED DEBRIS FLOW IN THE STUDY AREA

2.1 Debris Flows Sequence

Numerous debris flows in Beriti Hill, Bengkulu Province, Indonesia, caused damage to geothermal infrastructure, roads, water pipes, bridges, and houses during the 2016-2018 periods. The debris flows moved down to the Air Kotok River, causing the river elevation to be higher than the Air Karat and the Air Beras River. On 28 April 2016, a debris flow blocked the access road to the geothermal facilities. Moreover, on 13 December 2016, another flood occurred and carried sediment materials, blocking roads and eroding the drainage channel next to the Air Kotok Bridge. Further, floods occurred seven times from December 2017 to January 2018 due to the Cempaka and Dahlia tropical cyclones. The most significant flood occurred on 18 December 2017, damaging roads and geothermal pipes and eroding the riverbank downstream. The subsequent floods were relatively small and did not carry large sediment, thus only causing minor damage. Fig.1 shows the aerial map of the Air Kotok River and the observed field investigation location from various flash flood occurrences.

2.2 Geomorphological and Geological Setting

The geomorphological condition of the Air Kotok River from the upstream to the downstream is shown in Fig.1. The geomorphology of this river is an alluvial fan classified into four zones: *source area, upper fan, mid fan, and distal fan*, based on the deposition of the sediment supply. Each zone has different particle size characteristics, where the composing rocks found farther from the material source have more refined grains than the area close to the material source. The Air Kotok River is the main river in the alluvial fan with a repetitive sedimentation mechanism from the upstream of colluvial material. The Air Kotok River is an active distributary channel with a main sediment transportation channel in normal conditions.

The Air Kotok Bridge, located in the middle fan area, has a gentler slope than the upper fan. The debris flow material deposit in the middle fan area is shown in Fig.1. Several geomorphological parameters should be considered to determine the Sabo dam location, such as slope variation, alluvial

fan zone, braided channel in the alluvial fan zone, and the morphological condition.

In the mid fan, the Air Kotok River area comprises boulders and sandy material. The stratigraphic data shows a repetition of volcanic breccia layers with sandstones indicating the recurring events of debris flow in the area [23]. The area has a gentle slope (3° - 8°) with a drainage pattern of a braided channel. The active braided channel is located downstream and has constant flows all year. This section contains channel bars and point bars. In the upper fan area, the river is V-shaped and has a wide cross-section. The erosion has a vertical and lateral direction (Fig.2). Some part of the upper fan is identified as a potential source area and transported area. The lithology of the source area is andesite-basalt with a high weathering degree due to the hydrothermal alteration. The area is affected by the geological structure and, as a result, has steep slopes and high mass movement potential. The area has the potential to form natural weirs due to landslides that block active channels. The transported area is composed of rocks with boulders and sand material.

3. DEBRIS FLOW HAZARD ANALYSIS

3.1 Field Investigation

The river area near the bridge consists of rock that varies from gravel to boulder rocks. As observed during the field investigation, the river flow is relatively small. The subgrade color tends to be brown in the river channel, likely due to the chemical elements (sulfur or metals) carried along the river water. The area on the left and right banks of the river, where the Sabo dam will be built, is covered by dense deciduous forest and bushes. However, large-diameter trees are rarely seen in the area.

A soil investigation was carried out in the proposed construction area of the Sabo dam using the core drilling method and the Standard Penetration Test (SPT) at two boreholes, which locations are shown in Fig.1. From the drilling data at the Air Kotok River, BH-1 bore log shows a cyclic sedimentary mechanism in the middle of the water flow. In contrast, the BH-2 drilling log shows that the sedimentary cycle occurs in the middle fan - distal area alluvial fan. The density of soil layers in the area is medium to dense, with an SPT-N value of usually more than 20. The presence of gravel and rocks in the soil contributes to the value of SPT-N obtained during the test.

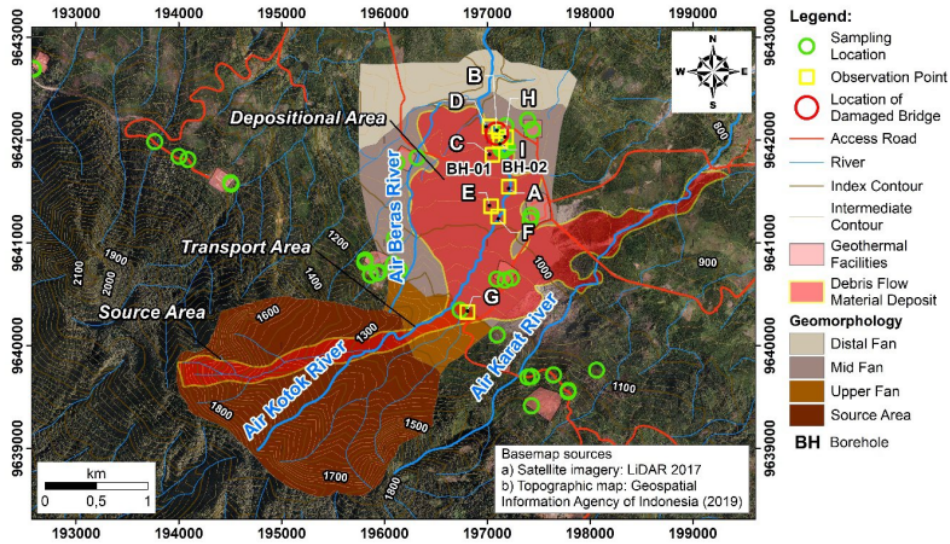


Fig.1 Topographical map of Air Kotok River and observation points (modified from LiDAR and [22])

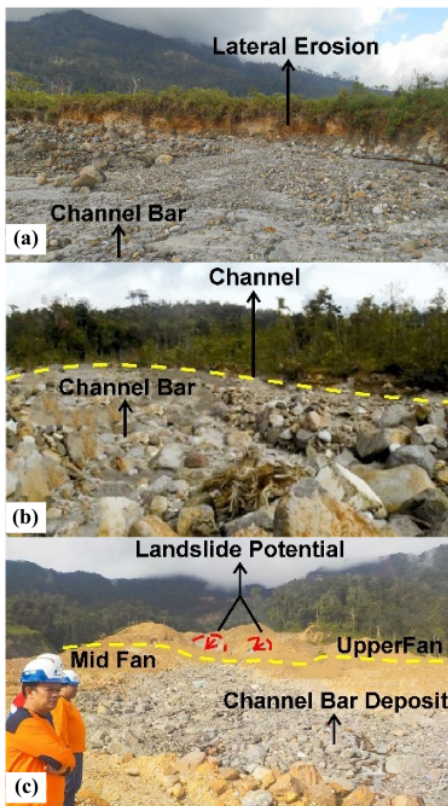


Fig.2 Channel bar and point bars formed after the debris flow occurrences in the middle fan area. (a)

and (b) the erosion near the Air Kotok Bridge. (c) the erosion near the transported area

Based on the investigation, the lithology condition is sediment materials from floods in the last few years. The deposited materials in the river are constituted of rock fragments with sizes ranging from gravel and boulder with sand deposits and clay/silt in the surrounding area. The rocky outcrop in the riverbank is a volcanic breccia, sandstone, and andesite (Fig.3).

The soil sample from the location of the designated Sabo dam comprises rocks with clay/silt or sand as a filler. The sample physical properties taken from the borehole have specific gravity values, ranging from 2.40 to 2.70. Although there are materials with a specific gravity of less than 2.50 because the material contains limestone or organic materials, those values are considered acceptable. The soil water content is generally less than 26%, likely because the sample was taken in the dry season. The fine material content is less than 36%, with low plasticity or non-plastic. With soil grain composition dominantly coarse fraction, referring to the Unified Classification System (USCS), the tested soil sample is mainly classified as SW, SP, and SM (sand to silty/clay with low plasticity). The soil shear strength with the direct shear test shows that soil cohesion (c) varies from 0 to 25 kN/m² with an internal friction angle (ϕ) of 30° to 40°.

3.2 Hazard Mapping

The debris flow material at the Beriti Hill area was andesite boulders and weathered volcanic breccia that traveled 2.5 km and damaged geothermal facilities. The debris flow volume on 28 April 2016, calculated based on the topography map before and after the landslide, reached 4,300,000 m³. The source of the landslide materials was three different caldera walls. The material movement of the caldera wall also eroded the valley walls, deepening the upstream and increasing the volume of landslide materials. The debris flow hazard map was derived from the field investigation and geological analysis.

The regional debris flow hazard analysis in the study area was carried out using GIS through a geological-geomorphological approach combined with the interpretation of satellite imagery [24]. The geology-geomorphology conditions such as topography, slopes, lithology, river stream, and catchment area determine the energy deposition and surface erosion during the debris flow occurrence. Debris flow deposits from the previous event were identified through LiDAR image changes between 2014 and 2017. The mainstream of the Air Kotok River was comprehensively evaluated using all of the available data that has been analyzed to produce a simplified regional debris flow hazard map.

The very high-risk zone of debris flow hazard is influenced by the steep morphology and consists of volcanic breccia and andesite lava. This zone shows the source of mass that has movement, especially in the crater area in the hills. The upstream part of the mainstream of Air Kotok River has a high potential to be affected by debris flow. The upstream became a transportation route with high depositional energy and a high erosion rate. The high-risk debris flow hazard zone is adjacent to the Air Kotok river's main channel, with lower energy deposition and erosion rates than the very high-risk zone. This is due to the morphological changes in this area, which include more moderate slopes. The medium-risk debris flow hazard zone is located downstream of the Air Kotok river's mainstream. The area around the alluvial fan falls into this zone, which has low depositional energy and erosion rates.

Based on the debris flow hazard map in the Air Kotok River and its surrounding area (Fig.4), the very high-risk zone is located in the source area of Beriti Hill. It is then followed by the high-risk zone downstream to the Air Kotok Bridge. The moderate risk zone ranges from the Air Kotok Bridge to the Bingin Kuning Bridge, 13 km downstream. The very high-risk zone indicates that the area will be affected mainly by debris flows. The scale of the

debris flow effect will gradually become smaller in the high-risk zone and even smaller in the moderate risk zone. The hyper-concentrated sediment is deposited in the sand pocket upstream of the bridge [25].

4. RESULT AND DISCUSSIONS

4.1 Conduit-type Sabo Bridge

Based on the geological and geomorphological assessment, the location of the Sabo dam is selected upstream of the damaged bridge. Fig.5 shows the Sabo bridge view from the upstream (cross-section A-A' in Fig.6). The river morphology that narrows downstream makes the selected location ideal for controlling sediment as the upstream location could be used as a sand pocket. In addition, several structural damages were found in the upstream and downstream areas near the Air Kotok Bridge. The debris flow eroded the supporting pillars and the foundation of the bridge. With a flow controller (in the form of a Sabo dam) from the upstream to the downstream of the Air Kotok River, the potential of Sabo bridge failure caused by abrasive flows is smaller.

The usage of the Sabo dam as a countermeasure of debris flow in Beriti Hill area has been proposed in the previous study, such as a series of Sabo dams with four main Sabo dams at Air Kotok River [26] and Conduit-types Sabo dam series with two main Sabo dam at Air Beras River [27]. In this study, the proposed mitigation of debris flow uses a single conduit type Sabo dam construction, whereas the upper side of the dam can function as an access road. The Sabo dam is completed with a sub-Sabo dam and an apron to support the stability of the main dam and capture and limit the volume of debris material passing the Air Kotok River.

The design of the Sabo bridge in the Air Kotok River considers the geological and geomorphological aspects, hydrological-hydraulic, and geotechnical analysis. The hydrological analysis is divided into frequency analysis, synthesis unit hydrograph, and design flood hydrograph analysis. The hydraulic analysis was employed to determine the dimension of the Sabo bridge slits and estimate the flood distribution in the Air Kotok River and the depth of the specific return period flood. The geotechnical analysis was conducted to analyze the main dam structure's external stability, including shear, overturning, and soil bearing capacity.

The Sabo dam height is calculated based on the assumption of sediment volume to be controlled, i.e., 1.1 to 1.2 million cubic meters. After a series of calculations, the height of the Sabo dam (H_d) is determined to be 16 m. The Sabo dam storage capacity is calculated by considering the parameters

such as river width, Sabo dam height, pre-construction riverbed slope, and design riverbed slope [28]. With the Sabo dam height (H_d) of 16 m,

the manageable sediment volume is 1,120,000 m³ which can be started to retain as far as 480 m from the upstream of the Sabo dam.

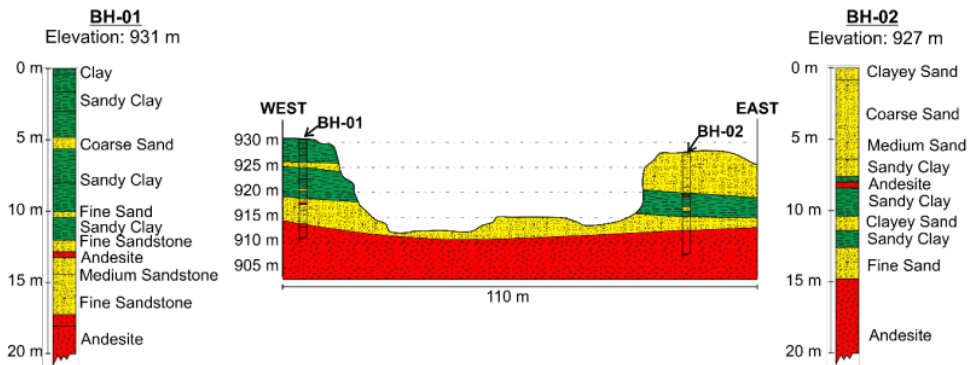


Fig.3 Stratigraphy at the river channel based on drilling log BH-01 and BH-02

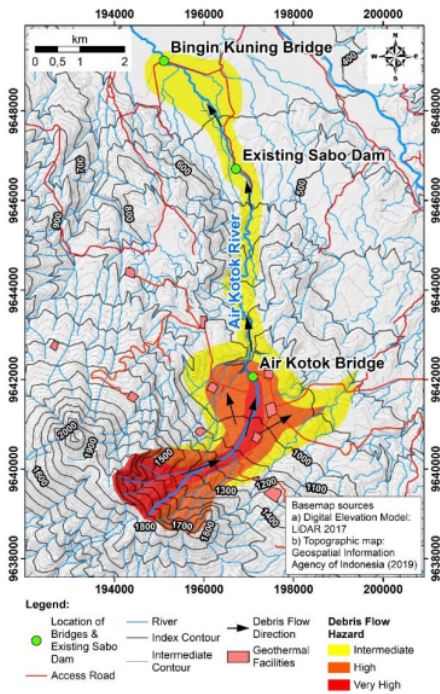


Fig.4 Debris flow hazard map at the study area Hydrology and Hydraulic Analysis

The hydrological analysis aims to calculate the design flood hydrograph according to the specified return period. The hydrograph is the result of the response of the watershed to design rainfall and is used to design the hydraulic structure of the Sabo dam. The frequency analysis is determined using spreadsheet software based on the annual maximum daily rainfall data for a certain period. The rainfall

data collection is based on satellite data from TRMM (Tropical Rainfall Measuring Mission). The data needed for the analysis are daily rainfall for the last ten years, which complies with the Indonesian National Standard [29,30]. The rainfall data used for the research is the data from 2001 to 2017. The Air Kotok watershed boundary is determined with WMS Version 10.1 software. It was found that the *output* area of the watershed is 3.77 km², the mainstream length is 4.02 km, and the average slope of the watershed is 0.72.

The Synthesis Unit hydrograph aims to determine the amount of flood discharge with watershed boundary data such as river length and riverbed slope [29,30]. The Synthesis Unit Hydrograph method suitable for the Air Kotok watershed is the Soil Conservation Service-Curve Number (SCS-CN), as this method considers the effects of land-use change. The design flood hydrograph analysis is carried out by multiplying the unit hydrograph and adequate rainfall [28]. The effective rainfall used is hourly rain according to the distribution of the frequency analysis results. A flood hydrograph based on the hydrological analysis results is then used to determine the safe hydraulic dimensions of the Sabo dam structure. A simulation was carried out with the HEC-RAS to see the distribution of floods along with the Air Kotok River flow from the flood hydrograph analysis.

The rainfall return period is determined with frequency analysis to select the type of distribution representing the distribution of maximum daily rainfall of the watershed. The frequency analysis uses spreadsheet software with four distributions of daily rain distribution: Normal, Log-Normal, Gumbel, and Log-Pearson III (Table 1). Referring to Chow et al. [28], the frequency analysis with two parameters, Chi-Squared and Smirnov-

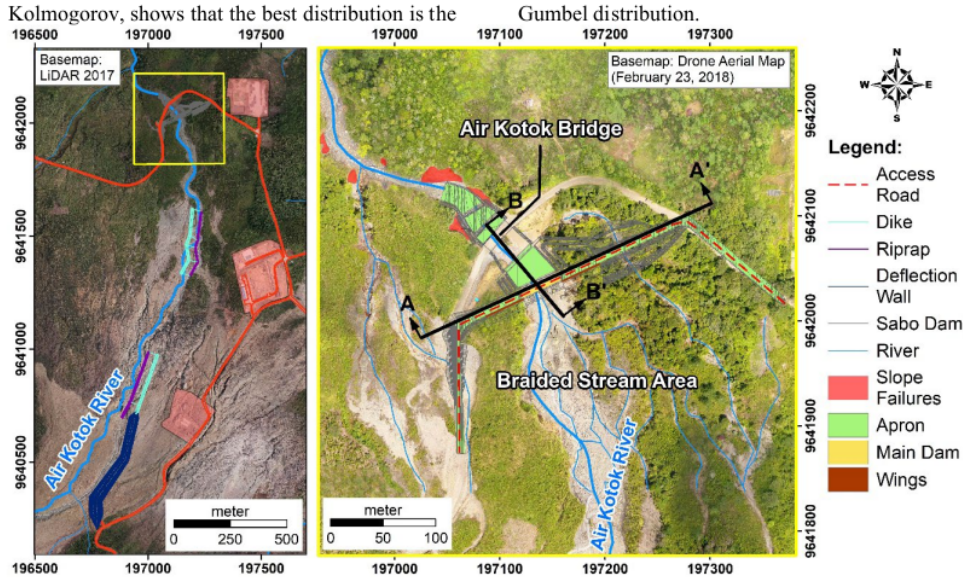


Fig.5 Selected location of the Sabo bridge from the 2017 LiDAR images (left) and drone aerial map (right)

4.2 Hydrology and Hydraulic Analysis

The flood discharge caused by the overflow of the Air Kotok River was analyzed using annual maximum daily rainfall data. The Air Kotok Watershed hydrological analysis calculated the design flood hydrograph obtained by multiplying the effective rain by the Soil Conservation Service-Curve (SCS-CN) unit hydrograph. The design flood discharge calculation used the Soil Conservation Service-Curve (SCS-CN) method; the discharge used for the Sabo dam design is the 100-year discharge. The 100-year flood hydrograph found that the design flood discharge (Q') value is 154.99 m^3/s . The design flood discharge can be transformed into the peak discharge of debris flow (Q_{sp}) using the Takahashi formula as follows:

$$Q_{sp} = \frac{C_s}{C_s - C_d} \times Q' \tag{1}$$

where the volumetric sediment concentration of the deposited sediment (C_s) is 0.6, and the volumetric sediment concentration of the moving sediment (C_d) is 0.3. If the riverbed slope is more than 20° , the concentration of debris flow is estimated by the following formula:

$$C_d = \frac{\rho \tan \theta}{(\sigma - \rho)(\tan \phi - \tan \theta)} \tag{2}$$

with σ is the density of big rock (kN/m^3), ρ is the water density (kN/m^3), ϕ is the internal friction angle of the deposited sediment ($^\circ$), and θ is the riverbed slope ($^\circ$). Based on Equations (1) and (2),

the value of the peak discharge of debris flow (Q_{sp}) is 309.98 m^3/s .

Debris flow velocity (v_{df}) is an important factor in the design of mitigation structures because it influences the impact forces (R), run-up, and superlevation of the flow (θ) [31]. Debris flow velocities are conventionally back-calculated from previous superlevation events [32] or predicted using the Equation below [33].

$$v_{df} = \frac{1}{n} R^{2/3} (\sin \theta)^{1/2} \tag{3}$$

Table 1 The analysis of design rainfall

Return period (year)	Normal (mm)	Log-Normal (mm)	Gumbel (mm)	Log-Pearson III (mm)
2	79.3	77.9	76.8	77.9
5	92.2	91.6	90.4	91.6
10	99.0	99.7	99.3	99.8
25	106.2	109.2	110.7	109.4
50	110.9	115.7	119.1	116.1
100	115.0	122.0	127.5	122.5

Based on Equation (3), the debris flows velocity reaches (v_{df}) 7.38 m/s. Therefore, the transported materials dissolve when transported down the slope. The depth of debris flow of 2.84 m is used to calculate the debris flow, water pressure, and the height of the Sabo dam opening.

The slits in the Sabo bridge are designed to allow the flood and debris flow to pass and allow sand and gravel to flow downstream during normal conditions to maintain sediment balance to prevent riverbed degradation. The spillway is designed to

resist the impact of sediments and scouring of the rocks that pass through it. The spillway width depends on the river width and the debris flow discharge. The main dam spillway thickness is determined based on the flow and gradation of the debris material, considering the possibility of damage due to debris impacts.

The Sabo dam opening is intended to drain flood and debris flows. The number of openings and dimensions is calculated based on Equation (4) by the trial-error method to obtain the optimal size and the number of openings. The maximum water level that passes through the opening (h_1) must not be greater than the height of the opening (H). The C is the coefficient of opening discharge, and B is the width of the opening.

The size and number of openings in the trial until the discharge (Q) through the openings is the same as the design discharge. The number of the slits is 6, the width of the opening (b) is 2.2 m, and the height of the opening (h_c) is 5.2 m.

$$Q = \frac{2}{15} C \sqrt{2g} (3B_1 + 2B_2) h_1^{1.5} \quad (4)$$

The designed height is safe from overflowing. The Sabo bridge is completed with a sub dam and apron, functioning as a trap for rocks, gravel, and sand so that they will not be transported downstream (Fig.6 (a)). The sub dam and apron will prevent the riverbed downstream of the Sabo dam

from being eroded by the debris flow from the Sabo bridge spillway. The apron structure protects the main dam from scouring downstream, maintaining the stability of the Sabo dam foundation and avoiding riverbank failure. The shape of the sub dam is adjusted to the shape of the main dam. The Sub dam height is a quarter of the main dam height [34,35].

Fig.6 (b) shows the dimension of the Sabo dam. The Sabo dam dimension design is determined using the calculation and peak discharge of debris flow and sediment volume to be controlled. The flood simulation used the HEC-RAS program, whereas the flood data input was performed based on the 100-year flood hydrograph analysis. The existing topography simulation shows that the flow moves to the access road and surrounding geothermal facilities (Fig. 7(a)). The result of the 100-year flood simulation after the Air Kotok River normalization by constructing the riprap, dikes, and Sabo dams downstream of the Air Kotok River (Fig. 7(b)) shows that the flood moves toward the Air Kotok Bridge. The overflow with small discharge can still occur and head to the access roads. The overflow can be diminished if the riprap and dikes are installed along the Air Kotok River. Water tunnels and drainages are installed along the access roads to prevent damage caused by overflow.

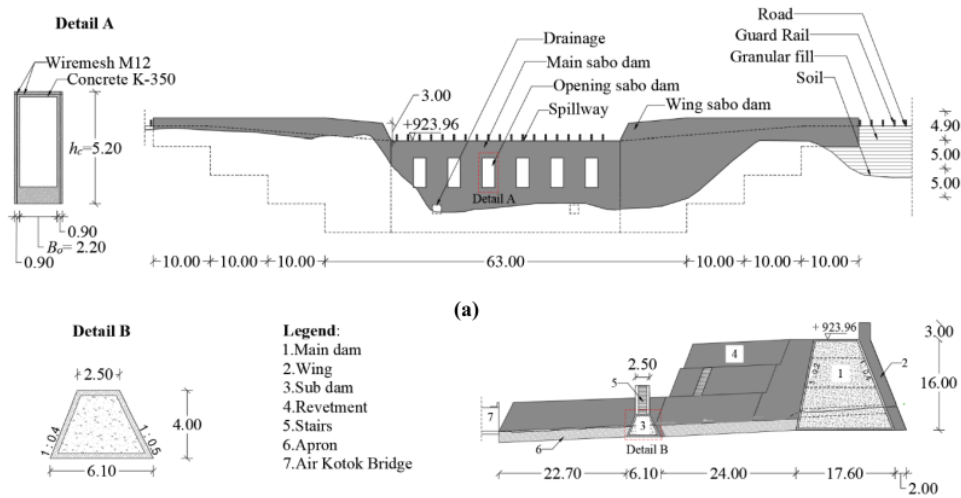


Fig.6 (a) Sabo bridge view from the upstream [Cross-section A-A' in Fig.5]; (b) Sabo dam dimension [Cross-section B-B' in Fig.5]

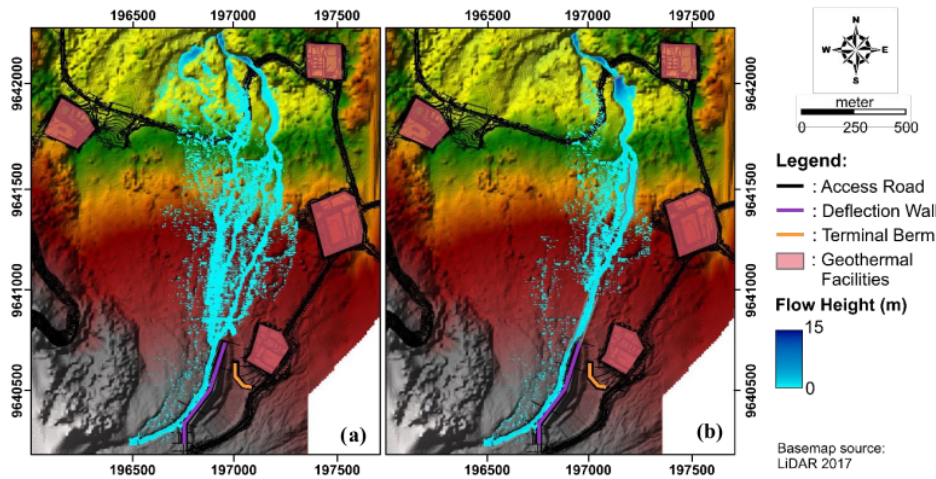


Fig. 7 Flood simulations with the 100-year return period are plotted in the 2017 LiDAR images. (a) Before normalization (existing condition). (b) After the normalization by constructing the rip rap and dikes upstream and Sabo dam downstream

4.3 Geotechnical Analysis

The data from the soil investigation results around the Sabo dam design location are used to analyze the stability of the Sabo dam structure. The main dam structure must withstand design loads that trigger structural failures such as dead load, static force, uplift, and hydrostatic. Overturning stability and sliding stability are calculated using the following equations:

$$SF_{\text{overturning}} = \frac{M_V}{M_H} \geq 2.00 \quad (4)$$

$$SF_{\text{sliding}} = \frac{F_V \tan \phi + cl}{F_H} \geq 1.5 \quad (5)$$

where M_V is the sum of the vertical moment, M_H is the sum of the horizontal moment, ϕ is the internal friction of soil, F_V is the vertical force, F_H is the horizontal force, c is the cohesion of soil, and l is the shear length.

The Sabo dam stability analysis considers external forces acting on the structure, as shown in Fig. 8 (a) and (b). The analysis is performed to evaluate the stability of the structure based on potential types of failure, namely stability against shearing, stability against overturning, and soil bearing capacity. The analysis method used complies with the Indonesian Standard SNI 2851:2015 [34] and the JICA [36]. Table 2 shows the results for the forces and moments acting on the Sabo dam during flood and debris flow.

Sliding failure occurs when the driving force is

higher than the resisting force. The resistance forces include hydrostatic pressure, Sabo dam gravity, lateral soil pressure, and shear strength (Table 3). Those forces are caused by hydrostatic pressure and structural weight. The value of the lateral soil coefficient is 0.32 with a cohesionless sedimentary soil type.

A structure may undergo overturning failure due to unbalanced moments acting on the structure. The moment is caused by acting forces multiplied by the moment arm to the center of overturning (Table 4). The soil test result at BH-1 is used to calculate the soil shear strength. The soil parameters with a depth of 2 m have an internal friction angle (ϕ) of 30.96° and cohesion (c) of 14.71 kN/m^2 . The obtained ultimate bearing capacity value is $4,486 \text{ kN/m}^2$. This value meets the requirement of the foundation bearing capacity for the Sabo dam.

During flood conditions, the external force acting on the main body is dominated by hydrostatic pressure. The hydrostatic pressure is divided into a horizontal force 16 m high, and a vertical force acts on the upstream and top of the Sabo dam. In addition, sliding resistance on the Sabo dam can be increased by the foundation soil's cohesive nature, which has a width of 17.6 m. On the other hand, in debris flow condition, the magnitude of the horizontal forces increase due to water pressure and lateral pressure on the sediment carried by the debris flow. Sediment materials are assumed to be located upstream of the main body with a slope of 2:5 and could act as a considerable moment resistance.

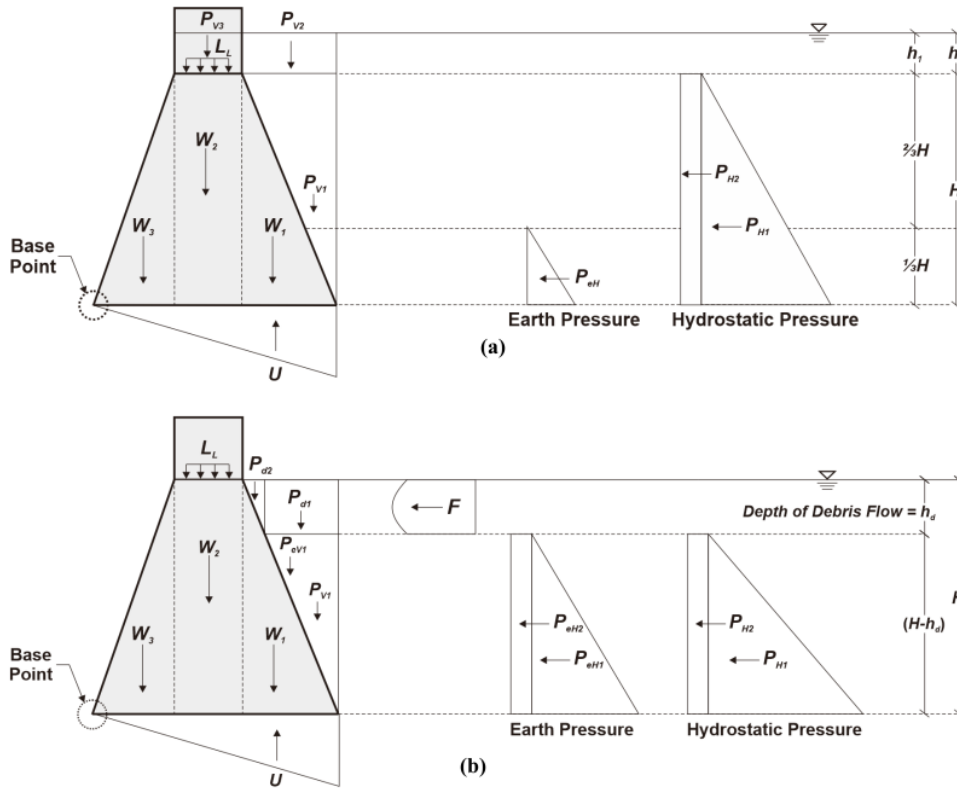


Fig. 8 External forces acted on the Sabo dam (Modified from JICA (2010)). (a) Flooding condition (b) Debris flow condition

Table 2 The calculation result of the forces and moments acting on the Sabo dam

Flood Conditions				
Loads	Force	Vertical Force (kN)	Horizontal Force (kN)	Moment (kN.m)
Dead load	W_1	1,229	-	16,384
	W_2	3,072	-	22,118
	W_3	614	-	1,311
Hydrostatic stress	P_{v1}	502	-	7,945
	P_{v2}	165	-	528
	P_{v3}	206	-	1,486
	P_{H1}	-	1,256	-6,697
Soil pressure	P_{H2}	-	413	-3,303
	P_{eH}	-	47	-250
Uplift	U	-1,608	-	-18,871
Live load	L_L	290	-	1,615
Total without L_L		4,181	1,715	20,651
Total with L_L		4,471	1,175	22,266

Debris Flow Conditions				
Loads	Force	Vertical Force (kN)	Horizontal Force (kN)	Moment (kN.m)
Dead load	W_1	1,229	-	16,384
	W_2	3,072	-	22,118
	W_3	614	-	1,311
Hydrostatic stress	P_{v1}	451	-	7,024
	P_{H1}	-	1,127	-5,696
	P_{H2}	-	125	-947
Soil pressure	P_{eV1}	473	-	7,375
	P_{eH1}	-	473	2,392
	P_{eH2}	-	186	1,408
Debris weight	P_{d1}	71	-	1,039
	P_{d2}	2	-	23
Water pressure	F_w	-	68	-1,054
Uplift	U	-1,309	-	-15,355
Live load	L_L	290	-	1,615
Total without L_L		4,604	1,979	28,421
Total with L_L		4,894	1,979	30,036

Table 3 Sliding stability of the Sabo dam

Flood Conditions			
Loads	Vertical Force (kN)	Horizontal Force (kN)	Safety Factor
Without Live Load	2,767	1,716	1.61
With Live Load	2,941	1,716	1.71
Debris Flow Conditions			
Without Live Load	3,021	1,979	1.53
With Live Load	3,195	1,979	1.61

Table 4 Overturning stability of the Sabo dam

Flood Conditions			
Loads	Vertical Moment (kNm)	Horizontal Moment (kNm)	Safety Factor
Without Live Load	30,902	10,250	3.01
With Live Load	32,517	10,250	3.17
Debris Flow Conditions			
Without Live Load	39,919	11,498	3.47
With Live Load	41,534	11,498	3.61

The sliding safety factor results tend to be smaller during the debris flow condition because of the additional forces from the water pressure and the lateral pressure from the sediment materials. The safety factor for overturning is higher during the debris flow condition because of the weight of the sediment materials that could act as a moment resistance upstream. The analysis also shows an increase in the safety factor for the condition with the live load. Live load is assumed to be the vehicles passing over the Sabo dam, which could increase the vertical forces acting above the Sabo dam structure. An increase in vertical forces will increase the moment resistance. Thus, the safety factor would also be increased.

5. CONCLUSIONS

The debris flow hazard map derived from the detailed debris flow hazard assessment shows that the study area has a very high, high, and medium risk of debris flow hazard. The very high-risk zone is located upstream of the Air Kotok River stream and followed by a high-risk zone downstream. The medium-risk zone is surrounded by the high-risk zone and continues through the Bingin Kuning bridge. Based on the field investigation, the geological and morphological conditions in the study area impact the debris flow risk potential.

The following conclusions are based on a

detailed analysis of engineering geology, hydrologic-hydraulic, and geotechnics. The design flood hydrograph with the Synthetic Unit Hydrograph Methods (HSS) Soil Conservation Service-Curve Number (SCS-CN) shows that the 100-year of flood design discharge (Q') is 154.99 m³/sec. The peak discharge of debris flow (Q_{sp}) is 285.12 m³/s. From the hydraulic aspect, a simulation using HEC-RAS without Sabo dam found that the debris flow will spread to larger areas upstream of the Air Kotok Bridge and destroy the structure of the old bridge. The proposed conduit Sabo dam and normalization of the Air Kotok river with riprap and dike resulted in more controlled debris flow distribution with sediment materials trapped in the storage area upstream of the Sabo dam.

This study proposes the Sabo dam design in Air Kotok River to have the following dimensions; the Sabo dam is 16 m high, the spillway is 8 m wide, and the wings on the right and left sides are 3.9 m high 2 m wide. This structure can manage 1,120,000 m³ of sediment. The Sabo dam has six openings with a height of 5.2 m and a width of 2.2 m, and two drainage holes with a dimension of 1.5 m × 1.5 m. The Sabo dam downstream is completed with an apron, a sub dam, and a sluiceway. The geotechnical point of view on the requirements of safe conditions against sliding and overturning risk are as follows; the value of the critical safety factor against sliding and overturning are 1.53 and 3.01, respectively. Based on the analysis, the subgrade has adequate bearing capacity to support the traffic loads. The results show that the design meets the safety requirement for sliding and overturning. Therefore, the designed closed-type conduit Sabo dam proposed in this study is capable, stable, and effective to be implemented as a mitigation measure to control and reduce the risk of debris flow.

6. ACKNOWLEDGMENTS

The authors would like to thank all the parties involved in this study for assisting in the field survey and data analyses. The authors would also like to thank the staff in the Soil Mechanics Laboratory in the Department of Civil and Environmental Engineering and Central Laboratory in the Department of Geological Engineering, Faculty of Engineering, Universitas Gadjah Mada for their support in laboratory testing. This research was funded by the Development Program of the Center for Excellence in Higher Education Science and Technology, Directorate General of Institutional Affairs of Science, Technology and Higher Education, Ministry of Research and Technology of the Republic of Indonesia, 2018-2019. Contract number: 227/401196/5698/11/2018 dated 24 February 2018 and contract number

204/401196/5698/III/2019 dated 4 March 2019.

7. REFERENCES

- [1] Kim, N., Nakagawa, H., Kawaike, K., & Zhang, H. (2012). Influence of a Series of Sabo Dams on Debris Flow Deposition. *DPRI Annuals*, 56, 531–538.
<https://ci.nii.ac.jp/naid/120005373015/en/>
- [2] Takahashi, T. (2009). A Review of Japanese Debris Flow Research. *International Journal of Erosion Control Engineering*, 2(1), 1–14.
<https://doi.org/10.13101/ijece.2.1>
- [3] Kim, N., Nakagawa, H., Kawaike, K., & Zhang, H. (2013). A Study on Debris Flow Deposition by The Arrangement of Sabo Dam. *Journal of Japan Society of Civil Engineers, Ser. B1 (Hydraulic Engineering)*, 69(4), 1_97-I_102.
https://doi.org/10.2208/jscejhe.69.I_97
- [4] Kim, N., Nakagawa, H., Kawaike, K., & Zhang, H. (2014). A study on debris flow outflow discharge at a series of Sabo dams. *Journal of Japan Society for Natural Disaster Science, JJSNDS*, 33, 43–52.
- [5] Hungr, O., Evans, S. G., Bovis, M. J., & Hutchinson, J. N. (2001). A review of the classification of landslides of the flow type. *Environmental and Engineering Geoscience*, 7(3), 221–238.
<https://doi.org/10.2113/gseegeosci.7.3.221>
- [6] VanDine, D. F., & Bovis, M. (2002). History and goals of Canadian debris flow research, a review. *Natural Hazards*, 26(1), 69–82.
<https://doi.org/https://doi.org/10.1023/A:1015220811211>
- [7] Zhou, G. G. D., Li, S., Song, D., Choi, C. E., & Chen, X. (2019). Depositional mechanisms and morphology of debris flow: physical modelling. *Landslides*, 16(2), 315–332.
<https://doi.org/10.1007/s10346-018-1095-9>
- [8] Sepúlveda, S. A., Moreiras, S. M., Lara, M., & Alfaro, A. (2015). Debris flows in the Andean ranges of central Chile and Argentina triggered by 2013 summer storms: characteristics and consequences. *Landslides*, 12(1), 115–133.
<https://doi.org/10.1007/s10346-014-0539-0>
- [9] Fan, R. L., Zhang, L. M., Wang, H. J., & Fan, X. M. (2018). Evolution of debris flow activities in Gaojiagou Ravine during 2008–2016 after the Wenchuan earthquake. *Engineering Geology*, 235(January), 1–10.
<https://doi.org/10.1016/j.enggeo.2018.01.017>
- [10] Kean, J. W., Staley, D. M., Lancaster, J. T., Rengers, F. K., Swanson, B. J., Coe, J. A., Hernandez, J. L., Sigman, A. J., Allstadt, K. E., & Lindsay, D. N. (2019). Inundation, flow dynamics, and damage in the 9 January 2018 Montecito debris-flow event, California, USA: Opportunities and challenges for post-wildfire risk assessment. *Geosphere*, 15(4), 1140–1163.
<https://doi.org/10.1130/GES02048.1>
- [11] John Twigg; Humanitarian Practice Network. (2015). Disaster Risk Reduction-Good Practice Review 9. Humanitarian Policy Network. <http://odihpn.org/wp-content/uploads/2011/06/GPR-9-web-string-1.pdf>
- [12] Huang, J., Li, X., Zhang, L., Li, Y., & Wang, P. (2020). Risk perception and management of debris flow hazards in the upper salween valley region: Implications for disaster risk reduction in marginalized mountain communities. *International Journal of Disaster Risk Reduction*, 51(August).
<https://doi.org/10.1016/j.ijdr.2020.101856>
- [13] Xiong, M., Meng, X., Wang, S., Guo, P., Li, Y., Chen, G., Qing, F., Cui, Z., & Zhao, Y. (2016). Effectiveness of debris flow mitigation strategies in mountainous regions. *Progress in Physical Geography: Earth and Environment*, 40(6), 768–793.
<https://doi.org/10.1177/0309133316655304>
- [14] Yuan, D., Liu, J., You, Y., Zhang, G., Wang, D., & Lin, Z. (2019). Experimental study on the performance characteristics of viscous debris flows with a grid-type dam for debris flow hazards mitigation. *Bulletin of Engineering Geology and the Environment*, 78(8), 5763–5774.
<https://doi.org/10.1007/s10064-019-01524-z>
- [15] Liu, F. Z., Xu, Q., Dong, X. J., Yu, B., Frost, J. D., & Li, H. J. (2017). Design and performance of a novel multi-function debris flow mitigation system in Wenjia Gully, Sichuan. *Landslides*, 14(6), 2089–2104.
<https://doi.org/10.1007/s10346-017-0849-0>
- [16] Johnson, P. A., & McCuen, R. H. (1990). Slit dam design for debris flow mitigation. *ASCE*, 115(9), 1293–1296.
[https://doi.org/10.1061/\(ASCE\)0733-9429\(1989\)115:9\(1293\)](https://doi.org/10.1061/(ASCE)0733-9429(1989)115:9(1293))
- [17] Hübl, J., Suda, J., Proske, D., Kaitna, R., & Scheidl, C. (2009). Debris Flow Impact Estimation. *International Symposium on Water Management and Hydraulic Engineering*, September, 137–148.
- [18] Banihabib, M. E., & Forghani, A. (2017). An assessment framework for the mitigation effects of check dams on debris flow. *Catena*, 152, 277–284.
<https://doi.org/10.1016/j.catena.2017.01.018>
- [19] Liu, W., Yan, S., & He, S. (2020). A simple method to evaluate the performance of an intercept dam for debris-flow mitigation. *Engineering Geology*, 276(July), 105771.
<https://doi.org/10.1016/j.enggeo.2020.105771>
- [20] Mizuyama, T. (2010). Recent Developments in Sabo Technology in Japan. *International Journal of Erosion Control Engineering*, 3(1), 1–3. <https://doi.org/10.13101/ijece.3.1>
- [21] Kim, Y., Nakagawa, H., Kawaike, K., & Zhang, H. (2017). Study on hydraulic characteristics of sabo dam with a flap

- structure for debris flow. *International Journal of Sediment Research*, 32(3), 452–464. <https://doi.org/10.1016/j.ijsrc.2017.05.001>
- [23] Geospatial Information Agency of Indonesia. Indonesia's digital topographic map 2015-2019. Scale Not Given. <https://tanahair.indonesia.go.id/portal-web/>. Accessed on March 2021
- [24] Wilopo, W., and Faisal Fathani, T. (2021). The mechanism of landslide-induced debris flow in Geothermal area, Bukit Barisan Mountains of Sumatra, Indonesia. *Journal of Applied Engineering Science*, 1–10. <https://doi.org/10.5937/jaes0-29741>
- [25] Hürlimann, M., Copons, R., & Altimir, J. (2006). Detailed debris flow hazard assessment in Andorra: A multidisciplinary approach. *Geomorphology*, 78(3–4), 359–372. <https://doi.org/10.1016/j.geomorph.2006.02.003>
- [26] Di Silvio, G. (1991). Soil erosion and conservation Part 2: Erosion control works.
- [27] Fajarwati, Y., Fathani, T. F., Faris, F., & Wilopo, W. (2020). Desain Sabo Dam Tipe Conduit Sebagai Pengendali Daya Rusak Aliran Debris. *Inersia: LNformasi Dan Ekspose Hasil Riset Teknik Sipil Dan Arsitektur*, 16(2), 105–116. <https://doi.org/10.21831/inersia.v16i2.36897>
- [28] Lestari, D. A., Fathani, T. F., Faris, F., & Wilopo, W. (2021). Designing conduit sabo dam series as a debris flow protection structure. *E3S Web of Conferences-The International Conference on Disaster Mitigation and Management*.
- [29] Chow, V. T., Maidment, D. R., & Mays, L. W. (1988). *Applied Hydrology* (Internatio). McGraw-Hill Book Company, New York.
- [30] SNI 2415:2016, "Calculation procedure for flood discharge plan," National Standardization Agency of Indonesia, 2016.
- [31] SNI 1724:2015, "Hydrological and hydraulic analyses and river building design criteria," National Standardization Agency of Indonesia, 2015.
- [32] Prochaska, A. B., Santi, P. M., Higgins, J. D., & Cannon, S. H. (2008). A study of methods to estimate debris flow velocity. *Landslides*, 5(4), 431–444. <https://doi.org/10.1007/s10346-008-0137-0>
- [33] AM, J. (1984). Debris flow in Brunsten: slope instability. In Willey (pp. 257–361).
- [34] Lo, D. O. K. (2000). Review of natural terrain landslide debris-resisting barrier design. In *GEO Report: Vol. No 104*.
- [35] SNI 2851:2015, "Design of sediment retention," National Standardization Agency of Indonesia, 2015.
- [36] Leonardi, A., Goodwin, G. R., & Pirulli, M. (2019). The force exerted by granular flows on slit dams. *Acta Geotechnica*, 14(6), 1949–1963. <https://doi.org/10.1007/s11440-019-00842-6>
- [37] JICA, "Technical Standards and Guidelines for Planning and Design of Sabo Structure," 2010.

Copyright © Int. J. of GEOMATE All rights reserved, including making copies unless permission is obtained from the copyright proprietors.

Debris Flow Hazard Analysis Toward The Implementation Of Mitigation Measures

ORIGINALITY REPORT

2%

SIMILARITY INDEX

2%

INTERNET SOURCES

0%

PUBLICATIONS

1%

STUDENT PAPERS

MATCH ALL SOURCES (ONLY SELECTED SOURCE PRINTED)

1%

★ Submitted to Politeknik Negeri Bandung

Student Paper

Exclude quotes On

Exclude matches < 1%

Exclude bibliography On